

# The evolution of galaxy clustering since $z = 3$ using the UKIDSS Ultra Deep Survey: the divergence of passive and star-forming galaxies

W. G. Hartley<sup>1\*</sup>, O. Almaini<sup>1</sup>, M. Cirasuolo<sup>2</sup>, S. Foucaud<sup>1,3</sup>, C. Simpson<sup>4</sup>,  
C. J. Conselice<sup>1</sup>, I. Smail<sup>5</sup>, R. J. McLure<sup>2</sup>, J. S. Dunlop<sup>2</sup>, R. W. Chuter<sup>1</sup>,  
S. Maddox<sup>1</sup>, K. P. Lane<sup>6</sup>, E. J. Bradshaw<sup>1</sup>

<sup>1</sup>*School of Physics and Astronomy, University of Nottingham, University Park, Nottingham NG7 2RD*

<sup>2</sup>*Institute for Astronomy, University of Edinburgh, Royal Observatory, Edinburgh EH9 3HJ*

<sup>3</sup>*Department of Earth Sciences, National Taiwan Normal University, No. 88, Section 4, Tingzhou Road, Wenshan District, Taipei 11677, Taiwan*

<sup>4</sup>*Astrophysics Research Institute, Liverpool John Moores University, Twelve Quays House, Egerton Wharf, Birkenhead CH41 1LD*

<sup>5</sup>*Institute for Computational Cosmology, Department of Physics, Durham University, Durham DH1 3LE*

<sup>6</sup>*Department of Astrophysics, University of Oxford, OX1 3RH*

## ABSTRACT

We use the UKIDSS Ultra-Deep Survey to trace the evolution of galaxy clustering to  $z = 3$ . Using photometric redshifts derived from data covering the wavelength range  $0.3 - 4.5\mu\text{m}$  we examine this clustering as a function of absolute K-band luminosity, colour and star-formation rate. Comparing the deprojected clustering amplitudes, we find that red galaxies are more strongly clustered than blue galaxies out to at least  $z = 1.5$ , irrespective of rest-frame K-band luminosity. We then construct passive and star-forming samples based on stellar age, colour and star-formation histories calculated from the best fitting templates. The clustering strength of star-forming galaxies declines steadily from  $r_0 \simeq 7h^{-1}\text{Mpc}$  at  $z \simeq 2$  to  $r_0 \simeq 3h^{-1}\text{Mpc}$  at  $z \simeq 0$ , while passive galaxies have clustering strengths up to a factor of two higher. Within the passive and star-forming subsamples, however, we find very little dependence of galaxy clustering on K-band luminosity. Galaxy ‘passivity’ appears to be the strongest indicator of clustering strength. We compare these clustering measurements with those predicted for dark matter halos and conclude that passive galaxies typically reside in halos of mass  $M \geq 10^{13}M_\odot$  while luminous star-forming galaxies occupy halos an order of magnitude less massive over the range  $0.5 < z < 1.5$ . The decline in the clustering strength of star-forming galaxies with decreasing redshift indicates a decline in the hosting halo mass for galaxies of a given luminosity. We find evidence for convergence of clustering in star-forming and passive galaxies around  $z \sim 2$ , which is consistent with this being the epoch at which the red sequence of galaxies becomes distinct.

**Key words:** Infrared: galaxies – Cosmology: large-scale structure – Galaxies: High Redshift – Galaxies: Evolution – Galaxies: Formation.

## 1 INTRODUCTION

The origin of the red sequence of galaxies, and more generally the bimodality in the colour-absolute magnitude plane (Visvanathan & Sandage 1977), have become increasingly important questions in extragalactic astronomy. Since Dressler (1980) first identified the trend for elliptical galaxies to be preferentially found in the denser regions of clusters, evidence has grown to

suggest that there are crucial differences in the evolutionary histories of red and blue galaxies at low redshift. Present day massive, passive galaxies are claimed to be largely in place by  $z=1$  or earlier (e.g. Yamada et al. 2005; Cimatti, Daddi, & Renzini 2006; Conselice et al. 2007), implying an extremely rapid period of star-formation. The luminosity and mass functions of lower-mass and star-forming galaxies, however, evolve significantly over the same time period (Bundy et al. 2006; Cirasuolo et al. 2010).

The early formation of stars in the most massive galaxies has become known as downsizing (Cowie et al. 1996) and is in contrast

\* E-mail: ppxwh1@nottingham.ac.uk

to the well-established hierarchical growth of the underlying dark matter distribution. These massive, quiescent galaxies dominate present-day groups and clusters and are thought to have formed at the highest peaks of the dark matter density field. The expected clustering of the dark matter is well understood (e.g. Mo & White 2002), and at any given epoch the real-space clustering amplitude over mid to large scales is a monotonically increasing function of dark matter halo mass. Measuring the clustering properties for galaxy samples therefore provides a direct link from the visible galaxies to the invisible dark matter in which they are found. Furthermore, the growth of dark matter halos over time is also well modelled, and so the evolution of the most massive systems throughout cosmic history can be traced through the use of clustering statistics.

Over the last few years the clustering technique has been applied to complete samples of optically-selected galaxies, separated by luminosity and colour. Zehavi et al. (2005) computed the angular auto-correlation functions of red and blue volume-limited sub-samples of galaxies from the Sloan Digital Sky Survey (SDSS; York et al. 2000) for separations  $< 10h^{-1}\text{Mpc}$  and redshifts,  $z < 1$ . They found that the population of galaxies red in  $g - r$  colour are more strongly clustered than those with bluer colours ( $r_0 = 5.7$  and  $3.6h^{-1}\text{Mpc}$  for red and blue populations respectively). Moreover, they show that this difference remains when the samples are further broken down into absolute R-band magnitude sub-samples.

Meneux et al. (2006) split the VIMOS-VLT Deep Survey (VVDS; Le Fèvre et al. 2005) galaxies into red and blue spectral types by the method of Zucca et al. (2006) and computed their clustering out to  $z \simeq 1.2$ . They found that the deprojected clustering scale length of the red spectral type galaxies ( $r_0 \sim 5h^{-1}\text{Mpc}$ ) was greater than that of the blue type galaxies ( $r_0 \sim 3h^{-1}\text{Mpc}$ ) at all redshifts investigated. Carlberg et al. (1997) find similar results for their sample at  $z \simeq 0.6$ . More recently Coil et al. (2008) used the DEEP2 galaxy redshift survey to address the same question at  $z = 1$ . They also found that red-sequence galaxies are more strongly clustered ( $r_0 \sim 5$  and  $3h^{-1}\text{Mpc}$  for red and blue samples), but additionally showed that those galaxies with intermediate colours had an intermediate clustering strength. They computed the relative bias between their sub-samples, finding a smoothly increasing bias with rest-frame (U-B) colour up to the red sequence.

Recently, two further deep surveys have been used to study the clustering of galaxies in the range  $0.2 < z < 1.2$ : the Canada-France-Hawaii Telescope Legacy Survey (CFHTLS; Ilbert et al. 2006) and the zCOSMOS field (Lilly et al. 2007). McCracken et al. (2008) used the CFHTLS, splitting the galaxy sample by template-fit spectral type and B-band luminosity. Based on photometric redshifts, they find that the difference in clustering strength between galaxies fit by early type and late type templates is roughly constant across all redshifts studied. The luminosity dependence at a given redshift, however, is minimal. Intriguingly, the early type population at  $z \sim 0.5$  shows hints of an inverse dependence of luminosity on clustering strength. The authors attribute this behaviour to fainter red galaxies being preferentially located in cluster environments. Meneux et al. (2009) meanwhile, use the spectroscopic zCOSMOS data, finding a weak dependence on luminosity which remains when stellar mass is used instead.

Each of these studies has been based upon an optical colour selection, which limits these studies to  $z \leq 1$ . Beyond this redshift optical studies become increasingly biased against passive and dusty galaxies and so are only able to probe the clustering of unobscured star-forming galaxies. The relative clustering strengths for

complete samples of passive and star-forming galaxies are therefore poorly understood beyond  $z \sim 1$ . Infrared survey data are not biased in this way and in addition, at  $z < 2$ , the K-band luminosity is a reasonable proxy for the stellar mass of a galaxy. Infrared-selected samples are therefore vital in the study of high redshift galaxy clustering.

Utilising infrared data, the high redshift progenitors of nearby high-mass, passive systems have been suggested as being passively-selected *BzK* galaxies (Daddi et al. 2004; Kong et al. 2006; Hartley et al. 2008), ultra-compact  $z=2$  red galaxies (e.g. Zirm et al. 2007; Toft et al. 2007; Cimatti et al. 2008), sub-mm galaxies (Lilly et al. 1999; Swinbank et al. 2006),  $24\mu\text{m}$  sources selected at  $z > 1$  (e.g. Magliocchetti et al. 2008), distant red galaxies (DRGs) (Franx et al. 2003; Conselice et al. 2007; Foucaud et al. 2007), extremely red objects (EROs) (Roche et al. 2002; McCarthy et al. 2004) and Ultra-luminous infrared galaxies (ULIRGS) (e.g. Farrah et al. 2006). Each of these populations have been found to cluster very strongly, with  $r_0$  values in the range  $7 < r_0 < 14h^{-1}\text{Mpc}$  (Roche et al. 2002; Blain et al. 2004; Farrah et al. 2006; Foucaud et al. 2007; Magliocchetti et al. 2008; Weiß et al. 2009).

In Hartley et al. (2008) (henceforth H08) we used the colour selection criteria of Daddi et al. (2004) to investigate the clustering properties of passive and star-forming galaxies at  $1.4 < z < 2.5$ . We showed that, when limiting the samples to  $K_{AB} < 23$ , the passive galaxies were significantly more clustered than star-forming galaxies. This result was found in angular clustering and also when deprojected to find the real-space clustering strength; with clustering scale lengths of  $\sim 15h^{-1}\text{Mpc}$  for the passive sample (pBzK) and  $\sim 7h^{-1}\text{Mpc}$  for the star-forming sample (sBzK).

Although all of these different galaxy populations overlap to some extent (Lane et al. 2007), their biases differ and they are sensitive to different epochs. It is therefore difficult to compare these samples with low redshift samples or to study global galaxy evolution. The analysis in H08 in particular left some open questions. We established that passive galaxies are more clustered even at such high redshifts, but the passive population is exclusively bright and the star-forming galaxies exhibited a strong limiting-magnitude dependence on clustering strength. It is therefore not clear whether it is luminosity or passivity that is more significantly correlated with clustering strength. Even at low-redshift debate remains over such a distinction (Norberg et al. 2002), complicated by the dominance of passive systems at the bright end of the luminosity function.

Williams et al. (2009) used a two-colour rest-frame selection to select a quiescent cloud and star-forming track over the range  $1 < z < 2$ . Using this novel selection, they compute the clustering scale lengths of their two samples, finding very similar lengths to those of the BzK selections in H08. They also report evidence for a mild evolution in clustering with luminosity for the star-forming galaxies by splitting their samples into two luminosity bins. Coil et al. (2006) also find, at  $z = 1$ , only a modest dependence for clustering strength to increase with B-band luminosity, covering  $0.7L^* < L < 1.4L^*$ .

A remaining open question is to determine when the passive population is built up. Though we found in H08 that this build-up occurs over  $1.4 < z < 2.5$ , and Williams et al. (2009) find similar evidence for their sample at  $1 < z < 2$ , these ranges in redshift are very broad. Can we identify a narrow epoch at which the clustering strengths of passive and star-forming galaxies of a given luminosity are equal? At this epoch passive and star-forming galaxies would occupy the same mass of dark matter halos and differences in their internal processes could be clearer. In this paper we attempt

to disentangle the effects on clustering strength due to passivity and luminosity and to further refine the redshift range over which the passive population of galaxies is first established.

Where relevant, we adopt a concordance cosmology in our analysis;  $\Omega_M = 0.3$ ,  $\Omega_\Lambda = 0.7$ ,  $h = H_0/100 = 0.7 \text{ km s}^{-1} \text{ Mpc}^{-1}$  and  $\sigma_8 = 0.9$ . All magnitudes are given in the Vega system unless otherwise stated. The remainder of the paper is organised in the following way: in the following section we provide details of the data sets used, derived quantities and method of selecting passive galaxies. In section 3 we compute the clustering strengths of these samples and then discuss their implications in section 4. We conclude in section 5.

## 2 DATA SETS, DERIVED QUANTITIES AND SAMPLE DEFINITIONS

The analysis we present in this work is based primarily on the third data release (DR3) of the ongoing UKIRT (United Kingdom Infra-Red Telescope) Infrared Deep Sky Survey, Ultra-Deep Survey (UKIDSS UDS, Lawrence et al. 2007). UKIDSS comprises five complementary sub-surveys with the UDS being the deepest, targeting a depth of  $K = 23$  over a single, 4-pointing mosaic of the Wide-Field Camera (WFCAM, Casali et al. 2007): an area of  $0.88 \times 0.88$  degrees. UKIDSS began in the spring of 2005 and the UDS has seen several data releases: an early release of the first few weeks of data (EDR, Dye et al. 2006), a one-year release (DR1, Warren et al. 2007), which we used in Hartley et al. (2008), and the more recent three-year data release (DR3).

The principle improvement from the DR1 to the DR3 is the addition of H-band data. Additional data in the K-band also provides an incremental improvement in depth. The  $5\sigma$  depths within  $2''$  diameter apertures for the DR3 in J, H and K-bands are 22.8 (AB 23.7), 22.1 (AB 23.5) and 21.8 (AB 23.7) respectively. These depths make it the deepest single-field near infrared survey of its area to date. For details of the stacking procedure, mosaicing, catalogue extraction and depth estimation we refer the reader to Almaini et al. (in prep.) and Foucaud et al. (2007).

In addition to near infrared data, the field is covered by extremely deep optical data in the B, V, R,  $i'$  and  $z'$ -bands from the Subaru-XMM Deep Survey (SXDS, Sekiguchi et al. 2005; Furusawa et al. 2008), *Spitzer* data reaching  $5\sigma$  depths of 24.2 and 24.0 (AB) at  $3.6\mu\text{m}$  and  $4.5\mu\text{m}$  respectively from a recent *Spitzer* Legacy Program (SpUDS, PI:Dunlop) and U-band data taken with CFHT Megacam. The SXDS utilised Suprimecam on the Subaru telescope, achieving depths of  $B_{AB} = 28.4$ ,  $V_{AB} = 27.8$ ,  $R_{AB} = 27.7$ ,  $i'_{AB} = 27.7$  and  $z'_{AB} = 26.7$  (Furusawa et al. 2008,  $3\sigma$ ,  $2''$ ). Border regions, areas around bright stars and obvious cross-talk artifacts were masked and any sources within such regions were discarded. The co-incident area with the UDS taking masking into account is  $0.63 \text{ deg}^2$ .

The world-public DR3 catalogue extracted from the K-band image is used as the basis for our selection, upon which we impose a cut at  $K = 21.1$  ( $K_{AB} = 23$ ) within  $2''$  diameter apertures. This cut was made to minimise photometric errors and the number of spurious sources and to ensure a high level of completeness and robust photometric redshifts (see below). This limit is fainter than  $M_K^*$ , the characteristic luminosity of the K-band luminosity function (Cirasuolo et al. 2010 and fig. 1). We are therefore probing the properties of ‘normal’ galaxies out to  $z = 3$ . Corresponding  $2''$  magnitudes for each object were extracted directly from the optical,

J and H-band images at the position of the source after a detailed astrometric re-alignment to the UDS K-band image.

From our combined catalogue we remove stars in the following way: bright ( $K < 18.1$ ) stars were removed by excluding those with K-band aperture magnitudes within  $3''$  and  $2''$  satisfying  $K_{3''} - K_{2''} > -0.14$ , where the stars are clearly separated from the galaxies. The remaining, fainter stars form a stellar locus in the  $(B - z') - (z' - K)$  plane (as noted by Daddi et al. 2004) and can easily be removed by the criterion  $(z' - K) < 0.3(B - z') - 0.5$  (Cirasuolo et al. 2010). Saturated stars and the surrounding contaminated regions were carefully masked out during the analysis. These cuts left 33923 galaxies from which we made our selections, as detailed in the following section.

The magnitudes obtained from the images were then used to determine photometric redshifts (photo-zs) and stellar ages by a  $\chi^2$  minimisation over a large suite of model templates, constructed using Bruzual & Charlot (2003) with a Salpeter initial mass function, and including a treatment of dust content (see Cirasuolo et al. 2007, 2010 for a full account). These templates cover nine values of the exponential star-formation decay rate ( $\tau = 0.1, 0.3, 0.5, 1, 2, 3, 5$  and 10 Gyrs, and an instantaneous burst), and allow stellar ages up to the age of the Universe at any given redshift. The dust reddening is allowed to vary between  $0 < A_V < 2$ , following the Calzetti law (Calzetti et al. 2000), and line of sight neutral Hydrogen absorption, calculated from Madau (1995), is also taken into account.

We remove from our catalogue any source with an unacceptable fit ( $\chi^2 > 15$ , 4.0% of the galaxy sample) as they will likely be mis-assigned when we break up our sample by redshift, and the derived stellar ages are unlikely to be reliable for such objects. Upon investigation, the majority of these discarded sources were found to be cross-talk artifacts (26%), QSOs (36%) or the minor members of pairs or mergers (23%). The majority of the remaining discarded objects were of very low surface brightness and many of them would not have made it into the volume-limited sub-samples. The fraction of otherwise useful objects rejected by this  $\chi^2 > 15$  criterion is therefore  $< 0.6\%$ . Rest-frame magnitudes and colours were computed by integrating the appropriate filter over the best-fitting template of each object. In this work we make use of the absolute rest-frame K-band magnitude and rest-frame  $(U - B)$  colour.

### 2.1 Sample selection

In this section we outline our definition of the passive galaxy sample. At low redshift, passive galaxies form a well-defined red sequence in a diagram of rest-frame  $U - B$  colour versus absolute magnitude. The red sequence is not exclusively composed of passive systems, however, and typically contains a 30% contamination from dusty star-forming galaxies (e.g. Wolf, Gray, & Meisenheimer 2005). At high redshifts ( $z > 1$ ) contamination by dusty star-forming objects becomes increasingly problematic (Daddi et al. 2004). In addition, a simple  $U - B$  cut does not make full use of all the available photometry. For these reasons, we define our passive sample with two criteria: (a) the galaxy must be ‘red’ in rest-frame  $U - B$  colour and (b) the best-fitting galaxy template must imply a very low level of residual star formation. These criteria are further detailed below.

Our rest-frame  $U - B$  colours are computed from the best-fitting template used to find the photometric redshift. The templates cover two possible star-formation histories: either an instantaneous burst parameterised by an age, or an exponentially decaying star-formation rate parameterised by an age and the e-folding time,  $\tau$ . Hence,

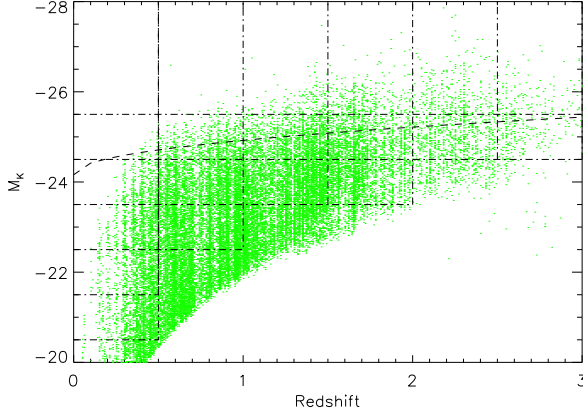


**Figure 1.** The distribution of UDS galaxies used in this work in the photometric redshift –  $M_K$  plane. The dot-dashed lines show the sub-sample regions for which we compute clustering lengths, provided they contain  $> 150$  galaxies. Also plotted, as the dashed-line curve, is the fit for the evolution of the characteristic luminosity,  $M_K^*$ , of the K-band luminosity function, as given in Cirasuolo et al. (2010).

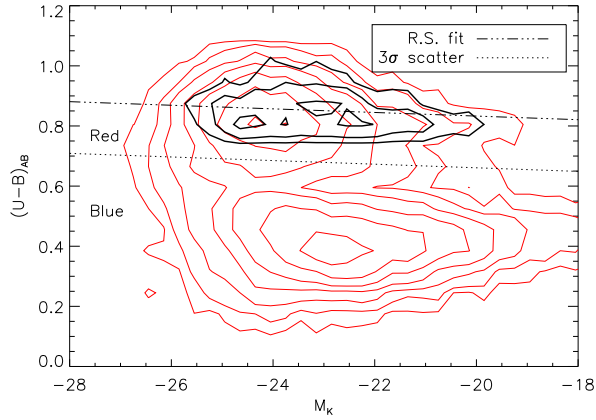


**Figure 2.** Colour-luminosity density plot of the full galaxy sample (light, red contours) and of those used to define the red sequence (heavy contours). The red sequence was defined by fitting a line of the form  $U - B = a \times M_K + b$  to the galaxies which were best fit by a burst template with age  $> 1$  Gyr. This fit is shown by the dot-dashed line, while the dotted line is the  $3\sigma$  lower envelope. Galaxies redder than the dotted line are defined as ‘red’ for the purposes of our sample selections.

$$SFR_{obs} = SFR_{initial} \times e^{-age/\tau} \quad (1)$$

where  $SFR_{obs}$  is the SFR at the time of observation.

We wish to define our red sequence initially using the most conservative and clean sample of passive galaxies drawn from our catalogue. We construct this sample to be those galaxies which are simultaneously old (age  $> 1$  Gyr) and are fit with a burst template, as these values imply a strong  $4000\text{\AA}$  break. We then perform a  $\chi^2$  minimisation to fit an equation of the form  $U - B_{AB} = a \times M_K + b$  to these galaxies. The ‘red’ sample is then taken to include all galaxies within  $3\sigma$  scatter of this fit (or redder). In Figure 2 we plot contours showing where galaxies lie in the  $(U - B)_{AB}$  vs. absolute K-band magnitude plane. Overlaid in black are the contours for

the burst galaxies described above, the associated best fit (dashed-dotted line) and red/blue selection criterion (dotted line).

The red sequence is known to evolve with time, with redder colours at lower redshifts (e.g. Brammer et al. 2009). Accurately accounting for this evolution with photometric redshifts is problematic. The typical errors on our  $U - B$  colours are 0.15 magnitudes, which is of the same order as the expected colour evolution. For simplicity, we choose not to treat the red sequence in such detail and instead use a fixed colour selection boundary. We note that our ‘red’ sample includes part of the green valley, and so we are unlikely to miss many intrinsically red galaxies at high redshift.

In order to remove the galaxies that are red due to dust rather than age we make use of the star-formation histories obtained from the templates. To be selected as a passive galaxy we require the galaxy to be red, as defined above, older than 1 Gyr and to have a best-fit SFR (from the photo- $z$  template fits) below some cut-off value (as given by equation 1, where  $\tau = 0$  for a burst model). By varying this SFR cut-off criterion we can study how the inclusion of galaxies with greater recent star formation rates influences the clustering strengths of the sub-samples.

We require, for our primary passive sample, a highly conservative limit to residual star-formation rate:  $SFR_o \leq 0.1\%$  of  $SFR_{initial}$  (in addition to being red in rest-frame  $U - B$  and with a stellar age  $> 1$  Gyr). We choose this strict limit to minimise the contamination by dusty star-forming objects whilst retaining sufficient objects with which to compute meaningful clustering lengths. There are well-known degeneracies between age, metallicity and dust content. We cannot completely overcome them, even with the multiple bands of deep photometry at our disposal. However, these parameters imply a strong break in the galaxy SED and hence only the most extreme dusty contaminants will be included. The number of objects satisfying these selection criteria is 3991 (33% of the ‘red’ sample). The vast majority of passive galaxies selected in this way also lie within the ‘pERO’ colour selection boundaries (see section 4).

We choose, as a baseline against which to compare our passive sample, an actively star-forming sample with a single criterion:  $SFR_o > 10\%$  of  $SFR_{initial}$ . This star-forming sample consists of 22856 objects of which 91% are ‘blue’ according to our  $(U - B)$  criterion and 9% are ‘red’. We then construct three further passive samples by relaxing the SFR criterion used in our primary passive sample to include galaxies with  $SFR_o \leq 0.5\%$ ,  $SFR_o \leq 1\%$  and  $SFR_o \leq 10\%$  of  $SFR_{initial}$ . In each of these three additional samples the requirements for red  $U - B$  colour and stellar age are kept the same as the primary sample. The number of objects in each of these expanded passive samples are 6111, 7677 and 10032 respectively. We will occasionally refer to these samples in the text by the SFR limit imposed during selection.

### 3 CLUSTERING PROPERTIES

The real-space correlation length of a sample of galaxies is intimately related to the mass of dark matter halos in which they are found. The value of this clustering scale-length is therefore of great interest in the study of galaxy formation and evolution. In this work we determine the angular correlation function of the galaxies as they are seen in projection, and then use the redshift distribution to deproject to find the real-space scale length ( $r_0$ ). This process is detailed below.

The 2-point angular correlation function,  $w(\theta)$  is defined by

the joint probability of finding two galaxies in solid angle elements  $\delta\Omega_1$  and  $\delta\Omega_2$  at a given separation (Peebles 1980),

$$\delta P = n^2 \delta\Omega_1 \delta\Omega_2 (1 + w(\theta_{12})). \quad (2)$$

To estimate the correlation function we use the estimator of Landy & Szalay (1993),

$$w(\theta) = \frac{DD - 2DR + RR}{RR} \quad (3)$$

where DD, DR and RR are the counts of data-data, data-random and random-random pairs respectively at angular separation  $\theta$ , normalised by the total number possible. Although this estimator is relatively robust against systematic errors, there remains a small bias due to the finite field size. This bias is corrected by an integral constraint, constant  $C$ . We follow the method of Roche & Eales (1999) by using the random-random counts to estimate the size of this bias:

$$C = \frac{\sum N_{RR}(\theta) \theta^{-0.8}}{\sum N_{RR}(\theta)}, \quad (4)$$

where the sums extend to the largest separations within the field.

The angular correlation functions are fit by  $\chi^2$  minimisation with a power law of fixed slope,  $\delta = -0.8$ . The fit is made over mid to large scales to avoid biases arising from multiple halo occupation. The small-scale limit corresponds to  $0.3h^{-1}\text{Mpc}^1$ , where previous  $w(\theta)$  measurements of galaxies over  $1 < z < 2$  begin to diverge from the large scale power law (H08). The large scale cut off is at 0.2 degrees where survey area limits our measurements. This method is the same as that presented in H08. Correlation function uncertainties are determined using bootstrap resampling, which are typically 2-3 times the Poisson errors.

The real space clustering and projected clustering are linked by the relativistic Limber equation (Limber 1954). If the redshift distribution of a sample is known, the Limber equation can be inverted and the correlation length,  $r_0$ , can be calculated in a robust manner (Peebles 1980; Magliocchetti & Maddox 1999; Roche, Dunlop, & Almaini 2003). Following Magliocchetti & Maddox (1999) and adjusting to take into account our known photometric redshift distributions we determine  $r_0$  as

$$r_0 = \left[ \frac{cA}{H_0 H_\gamma} \left( \frac{(\int_0^\infty n(z) dz)^2}{\int_0^\infty n(z)^2 x(z)^{1-\gamma} P(\Omega_0, z) F(z) dz} \right) \right]^{1/\gamma} \quad (5)$$

where  $n(z)$  is the redshift distribution of the sub-sample and all other symbols have the same meanings as in Magliocchetti & Maddox (1999).

Below we present the resulting measurements for  $r_0$  as a function of redshift and K-band luminosity. This is first determined for all galaxies and then further subdivided by colour and star-formation history.

### 3.1 The global evolution of clustering

Using the method outlined above we computed the galaxy clustering scale lengths,  $r_0$ , for each of the volume limited sub-samples shown in Figure 1, provided that each subsample contained at least 150 galaxies. These measurements are shown in Figure 3. The first

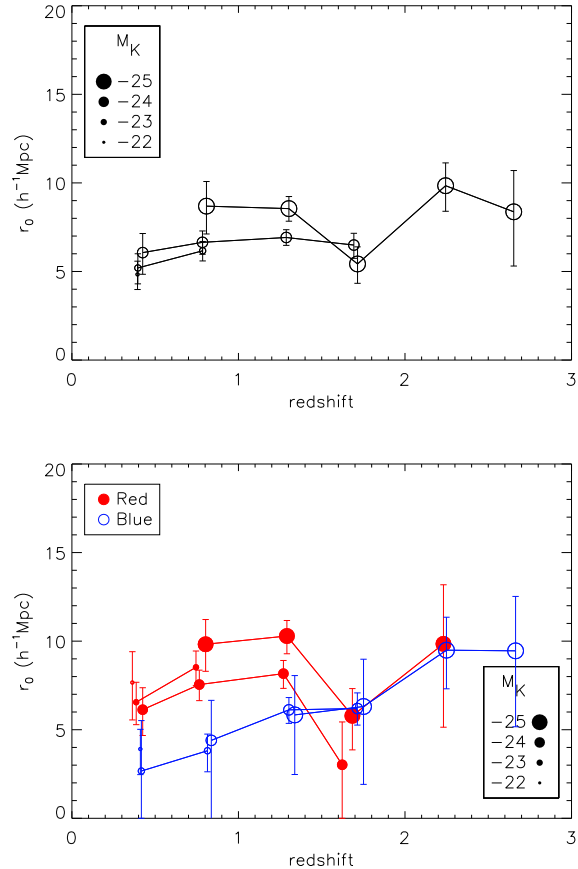


**Figure 3. Upper.** The global evolution of clustering in the UDS field. Galaxies are split into the volume-limited sub-samples shown in Figure 1 and the real-space correlation lengths are computed (see text). The evolution of clustering strength with redshift is mild for most luminosity ranges. **Lower.** The sub-samples are further separated into red and blue in rest-frame ( $U - B$ ) colour and the clustering computed once again. Globally, red galaxies are slightly more strongly clustered than blue galaxies. The increase in  $r_0$  found for bright galaxies at low-redshift is clearly seen to be dominated by red galaxies.

thing of note in these measurements is the lack of strong evolution of  $r_0$  with redshift at a given  $M_K$ . Furthermore, there is very little luminosity segregation, consistent with the findings of Coil et al. (2008), although the most luminous galaxies are slightly more strongly clustered at  $z \sim 1$ .

### 3.2 Colour and star-formation rate dependant clustering

In much of the literature concerning the evolution of galaxy clustering, populations are separated by colour, rather than star-formation properties. Rest-frame colours are simpler to compute and therefore allow more straightforward comparisons with previous work. In Figure 3 we again compute  $r_0$  values for the subsamples in Figure 1, but this time we also separate red and blue galaxies, using our rest-frame ( $U - B$ ) colours defined in Section 2.1 (Figure 2).

At  $z < 1$ , red galaxies are significantly more clustered than blue galaxies, similar to the result of Coil et al. (2008) at  $z \approx 1$ . This difference is particularly pronounced for the brightest sub-samples, where the strong clustering observed in the full sample is

<sup>1</sup> This value was chosen to maximise the fitting range, though we have also tried  $0.5h^{-1}\text{Mpc}$  and  $1.0h^{-1}\text{Mpc}$ , finding consistent results.

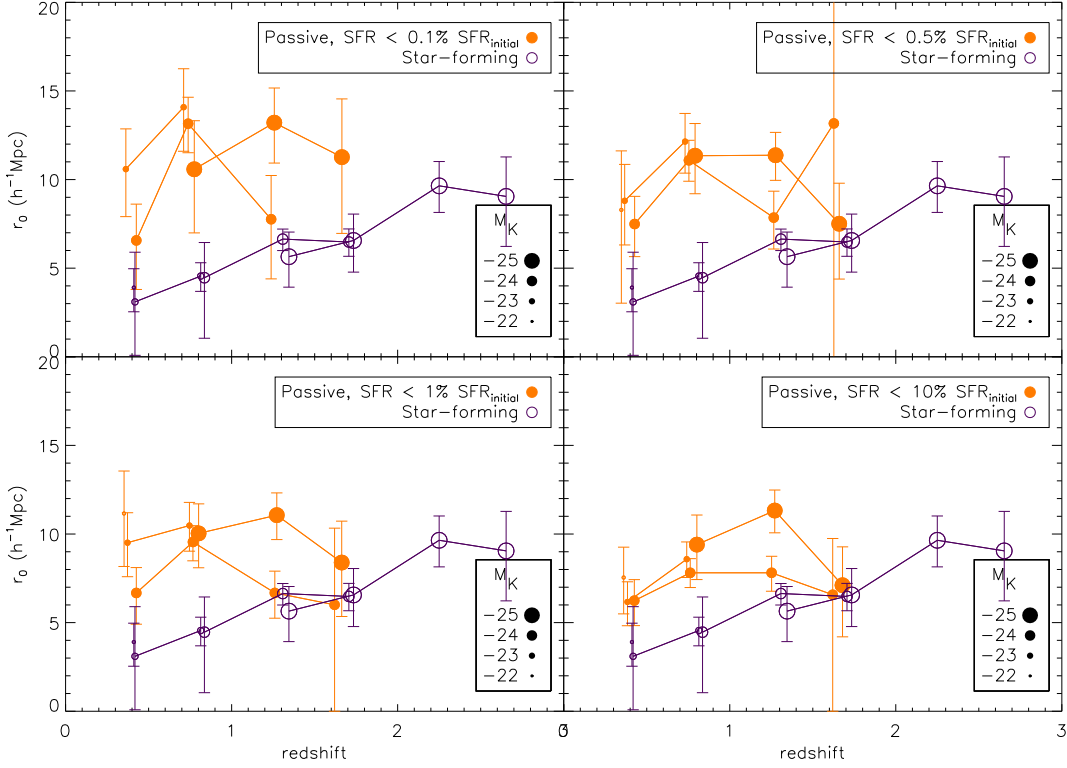


**Figure 4.** Evolution of the clustering strengths with redshift for our four passive samples with the single comparison star-forming sample. With the most conservative passive definition (requiring red rest-frame  $U - B$  colour, stellar age  $> 1$  Gyr and  $SFR_o \leq 0.1\% SFR_{initial}$ ), the passive galaxy sub-samples are significantly more strongly clustered than the star-forming sub-samples for  $z < 1.5$ . Above  $z = 2$  the number of passive galaxies becomes too small to make robust clustering measurements. As the passive galaxy selection criterion of SFR (given in each panel) is relaxed, the clustering strengths of star-forming and passive sub-samples become more similar. Each point is plotted at the mean redshift of the sub-sample it represents.

clearly a result of the clustering of red galaxies. Above  $z = 1.5$  the clustering strengths of the blue and red subsamples appear to converge, indicating that this may be the principle epoch at which the red sequence is populated. The red population is inhomogeneous, however, containing both passive and dusty star-forming objects. We therefore use our template fits to separate the passive and star-forming galaxies (Section 2.1).

We plot the deprojected clustering lengths of our passive and star-forming samples in Figure 4 with the SFR limits described in section 2.1 shown in each panel. For the most conservative passive sample ( $SFR \leq 0.1\%$ ) the clustering strengths of the passively-selected galaxies are greater than those of the equivalent star-forming galaxies for almost all sub-samples up to  $z = 1.5$ . Our result, shown in the upper left panel of Figure 4, shows that the clustering length is more strongly dependent on passivity than on luminosity, with very little luminosity segregation in the star-forming sample. This difference continues to at least the median redshift of BzK-selected galaxies (Hartley et al. 2008). Above  $z \sim 1.5$ , however, the respective clustering strengths of passive and star-forming galaxies appear to converge. Further survey data will be required to confirm this finding, which is discussed in section 4. As we relax the SFR requirement to allow galaxies with higher residual star-formation rates into the passive selection, we find that the strength of clustering of the passive sub-samples decreases, which confirms that truly passive galaxies are more strongly clustered among the ‘red’ population.

For illustration, in Figure 5 we show the angular clustering measurements for passive and star-forming galaxies over all sub-samples in the two redshift ranges,  $1 < z \leq 1.5$  and  $1.5 < z \leq 2$ . The passive samples use our conservative definition ( $SFR_o \leq 0.1\% SFR_{initial}$ ) described in section 2.1. The solid lines are the best power-law fits and, in agreement with our earlier measurements for BzK-selected galaxies (H08), the passive galaxies are found to cluster more strongly.

### 3.3 Comparison with modelled halo masses

We use the formalism given in Mo & White (2002) to find the clustering strengths of dark matter halos of given masses as a function of redshift. These models gather together previous work (Press & Schechter 1974; Bond et al. 1991; Mo & White 1996; Jing 1998; Sheth, Mo, & Tormen 2001) and use the ellipsoidal collapse model which has been calibrated against dark-matter only N-body simulations. Their aim is to provide the abundances and clustering of dark matter halos as functions of redshift and mass across a wide dynamic range.

In Figure 6 we plot these models for halos of mass  $10^{10} M_\odot$  to  $10^{14} M_\odot$  together with the results from our conservative passive sample (see section 2.1) and star-forming sample. At  $z < 2$ , star-forming galaxies generally occupy halos of mass  $10^{12} M_\odot$  or smaller, while passive galaxies occupy halos of mass  $10^{13} M_\odot$  to  $5 \times 10^{13} M_\odot$ . The general trend for star-forming galaxies is for



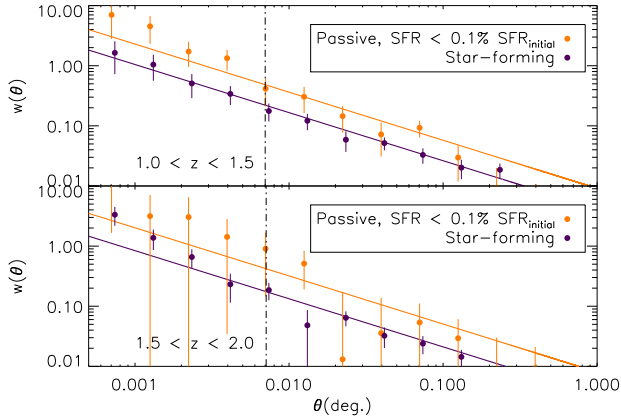


**Figure 5.** Angular clustering measurements for conservative passive galaxies ( $SFR_0 \leq 0.1\% SFR_{\text{initial}}$ ) and star-forming galaxies within the redshift ranges  $1 < z \leq 1.5$  (upper) and  $1.5 < z \leq 2$  (lower) with the star-forming points off set for clarity. Subsamples in luminosity have been combined for illustrative purposes. Solid lines show the best power-law fits, using a constant slope of  $-0.8$ , over large-scales:  $0.3 h^{-1}\text{Mpc}$  (Dashedline)  $- 0.2$  deg. In both cases the passive samples are more strongly clustered, consistent with the measurements of pBzK and sBzK-selected galaxies (e.g. H08). Errors are determined from a bootstrap analysis.

galaxies of a given luminosity to occupy halos of greater mass at higher redshift. This is a manifestation of halo downsizing (Cowie et al. 1996; Foucaud et al. 2010, in press). This downsizing in host halo mass for star-forming galaxies appears to extend beyond  $z=2$ . At these very early times bright star-forming galaxies are hosted by massive dark matter halos ( $M \sim 5 \times 10^{12} M_{\odot}$ ). Presumably these are among the progenitors of low redshift group-dominant galaxies.

The passive galaxies occupy halos up to an order of magnitude more massive than the star-forming galaxies. In contrast to the star-forming galaxies, the brightest passive galaxies appear to show constant clustering strength over the range  $0.5 < z < 1.5$ . If confirmed by future survey data, this result suggests that bright passive galaxies are hosted by similar mass halos across this redshift range.

#### 4 DISCUSSION

We have shown that passive galaxies, defined by fitting templates over 11 bands from the UV to *Spitzer's* IRAC bands, are more strongly clustered than star-forming galaxies at  $z < 1.5$ . Clustering strength is intimately linked with the minimum mass of dark matter halo that can host a galaxy of a given type. Passive galaxies therefore on average occupy more massive dark matter halos than their star-forming counterparts. These results indicate that at  $z < 1.5$  the passivity of a galaxy sample is a strong indicator of the typical mass of dark matter halo that host them.

The K-band luminosity is a reasonable proxy for the stellar mass of a galaxy, though galaxies may dim by approximately one magnitude after they stop forming stars (e.g. Lilly & Longair 1984; Cowie et al. 1996). Even taking this dimming into account, the conservative passive sub-samples ( $SFR \leq 0.1\% SFR_{\text{initial}}$ ) are typically more strongly clustered than the star-forming samples for a given stellar mass.

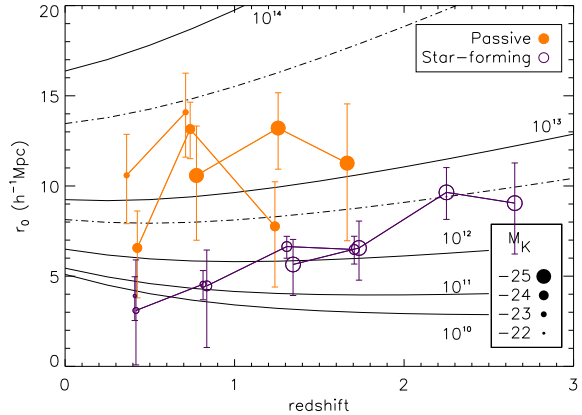


**Figure 6.** The clustering of our conservative passive sample and star-forming sample (symbols have the same meanings as in Figure 4) are compared with the clustering predictions of dark matter halos from Mo & White (2002). Lines of constant halo mass (in  $M_{\odot}$ ) are shown, with additional dashed-dotted lines for  $5 \times 10^{13} M_{\odot}$  (upper) and  $5 \times 10^{12} M_{\odot}$  (lower). Downsizing in the star-forming population is evident with the same luminosity galaxies found in less massive halos towards  $z=0$ . The same cannot be said of the passive galaxies, which typically occupy halos of mass  $M \geq 10^{13} M_{\odot}$ .

Furthermore, there is an absence of a strong luminosity dependence on the clustering strength of the star-forming samples. We have therefore found that of the two effects that we set out to disentangle, passivity and luminosity, passivity is the more significant indicator of clustering strength at  $z < 1.5$ . However, we note that we are unable to probe the most extreme high luminosity galaxies ( $M_K < -26$ ) due to our limited survey area.

Above  $z = 1.5$  we are unable to significantly distinguish star-forming and passive galaxy clustering. The correlation lengths of passive and star-forming galaxies apparently converge at this epoch. If this behaviour is confirmed it would suggest that the epoch  $z \sim 2$  is the epoch in which the passive and star-forming samples are first becoming distinct. Hence, it is likely to be the major epoch at which the red sequence is being populated. This finding makes the further study of the  $1.5 < z < 2.5$  range critical and we intend to return to and improve upon this work as the UDS data push deeper and spectroscopic samples become available.

In the hierarchical formation of structure the first halos to collapse are those which eventually merge to form the most massive halos at low redshifts. Our result then points towards a time sequence: passive galaxies formed earlier in those first halos while those of similar stellar mass, but still forming stars, developed in lower mass halos that collapsed later. Galaxy and halo evolution is accelerated at the earliest epochs with respect to the present day. The galaxies formed at these strongly clustered, high density peaks of the matter distribution are therefore likely to become fully evolved, passive galaxies more rapidly than the general population. Discounting mergers, the stellar mass of a galaxy is limited by the available gas reservoir so a passive galaxy could have formed significantly earlier than a star-forming galaxy, but end up with very similar stellar masses at the epoch of observation. Their respective halos, however, will have built-up mass since they first collapsed and so those of the earlier formers will be more massive. In this way the difference in clustering strength is a natural result of hi-

erarchical mass assembly in halos and downsizing in galaxies (c.f. Foucaud et al. 2010, in press).

In addition to the relative differences in clustering strength at a fixed redshift, we also find a potential difference in how the passive and star-forming samples evolve with redshift. The star-forming samples follow the behaviour we would expect as a result of the downsizing scenario for galaxy evolution. Sub-samples of a given K-band luminosity (stellar mass) taken from this population exhibit a decline in clustering strength towards  $z = 0$ . The most luminous *passive* galaxies show tentative evidence for constant clustering strength across  $0.5 < z < 1.5$ . A constant value of  $r_0$  of such magnitude indicates that the hosting dark matter halos are no less massive at lower redshift.

Direct comparison with the results of previous work is extremely difficult as the UDS is currently unique and this study is the first of its type utilising K-band selection. Qualitatively, our results agree very well with the findings of Coil et al. (2008), McCracken et al. (2008) and Meneux et al. (2006): each of these studies finds a longer clustering lengths for red or passive galaxies over blue or star-forming galaxies below  $z = 1$ . We furthermore agree with previous works that any luminosity dependence on clustering in the sample is minimal in comparison with that of passivity over the range of galaxy properties that we have investigated.

McCracken et al. (2008) find that at intermediate redshifts ( $0.5 < z < 1$ ), galaxies fit by an early-type template possibly have a inverse luminosity dependence, with less luminous galaxies having slightly longer correlation lengths. This behaviour is well known at low redshift, where passive dwarf galaxies exhibit strong clustering and are found to be associated with clusters of galaxies (Conselice et al. 2003; Zehavi et al. 2005). Our measurements for red galaxies at  $z < 1$  are not inconsistent with these findings.

#### 4.1 Discussion of uncertainties

Throughout this work there are uncertainties that are extremely difficult to quantify. Though dust attenuation is taken into account during template fitting, there is a well-established degeneracy between the stellar age and dust content. Even with the wide range of photometry available, we cannot fully overcome this degeneracy. In addition, the typical redshift uncertainties are  $\sim 0.05(1+z)$  and typical uncertainties in U-B colour are 0.15 magnitudes. We use the ERO definitions of Pozzetti & Mannucci (2000) to examine whether our passive selection method is robust. Each of the passive objects with best-fit redshifts within the range  $1 < z \leq 2$  meets the  $i - K > 4$  (Vega) ERO criterion, with 1423 of the 1457 objects lying in the passive ERO (pERO) region, defined by i,J,K colours. In addition, when plotted in the  $(B - z)_{AB} - (z - K)_{AB}$  plane, our conservative passive sample populates the areas in which we would expect to find passive galaxies (see the Appendix, Figure 7 and Lane et al. 2007). We are therefore confident that the SED-fit star formation properties we use are relatively robust, in comparison with previous broad band techniques.

Even with robust colours and selection criteria, the photometric redshift technique can introduce uncertainties into our measurements by causing a galaxy to be assigned to the wrong sub-sample in redshift. Passive galaxies have a strong break implied by our selection process and hence the photometric redshift determination is more reliable for these galaxies than for star-forming galaxies. There is an ongoing ESO Large Programme, the UDSz survey, to obtain  $\sim 4000$  redshifts of galaxies at  $z > 1$  in the UDS field. Early indications suggest that the photometric redshifts for our passive galaxies are indeed highly reliable, with error estimates of

$\delta_z \sim 0.02(1+z)$  (though at the time of writing the majority of these are at  $z < 1.75$ ).

Photometric redshifts are particularly difficult to obtain at  $z > 1.5$ . It is precisely beyond this point that the red and blue samples converge, due in part to a decrease in the red galaxy clustering. On the other hand, the blue and star-forming samples' clustering strengths increase over this range. Sub-sample misassignment, particularly in redshift, will tend to dilute the clustering signal. For the observed convergence to be driven by errors in the photometric redshifts would therefore require the clustering signal from our red sample to be washed out, while that from the blue sample is not. This in turn would require the redshifts of our blue and star-forming galaxies to be much more accurate than our red galaxies. We suggest that such a case is highly unlikely, but await a substantial sample of redshifts to confirm this.

Of greater concern is the possibility that due to photometric redshift errors, star-forming galaxies are more likely to be assigned to the wrong redshift bins. This would dilute the clustering of the blue galaxies and artificially enhance the difference between passive and star-forming samples. If dilution due to redshift errors is significant we might expect that our clustering measurements for star-forming galaxies are smaller than other studies of star-forming galaxies at these redshifts. In H08 the clustering strength of sBzK-selected galaxies for a sample of median redshift  $\sim 1.5$  cut at  $K = 23$  was found to be  $\sim 6.75 h^{-1} \text{Mpc}$ . This value is similar to the star-forming sub-samples of similar redshifts presented here. Although selections in other bands are not directly comparable we have found that clustering strength is only weakly dependent on K-band luminosity. Any moderately bright star-forming sample can therefore be used as a comparison. Coil et al. (2008) found that star-forming galaxies at  $z = 1$  have modest clustering strengths of  $\sim 4h^{-1} \text{Mpc}$ , with similar values found by Adelberger et al. (2004) (BM/BX-selected galaxies,  $z = 1$ ) and McCracken et al. (2008) ( $z = 0.6$ ). The  $z = 1$ , UV-selected galaxies in Heinis et al. (2007) have a slightly larger correlation length ( $4.1h^{-1} \text{Mpc} < r_0 < 5.5h^{-1} \text{Mpc}$ ), similar to those we report. At similar redshifts we find slightly longer ( $3h^{-1} \text{Mpc} < r_0 < 5h^{-1} \text{Mpc}$ ), but consistent, correlation lengths compared with most other studies.

A second method we can use to test this potential issue was also used in Magliocchetti & Maddox (1999). Magliocchetti & Maddox (1999) noted that there is a systematic error introduced into the  $r_0$  values when it is assumed that the redshift distribution is accurately known. They take account of this error by assuming the errors in the redshifts of their sub-samples are Gaussian random and apply a co-efficient,  $[(12\sigma^2/\Delta z^2) + 1]^{1/2\gamma}$ , to broaden the redshift distribution. In this work modelling the individual  $n(z)$  bins as top-hat functions would be inaccurate and so we have not attempted to adjust our  $r_0$  measurements in this way. However, this method can still provide an estimate of whether our result is driven by redshift errors. Each galaxy has an associated error in redshift, derived from the  $\chi^2$  distribution, which we assume here can be represented by a simple Gaussian. In this way each galaxy in a sub-sample has a probability of being at a given redshift and these individual probabilities are then binned and summed for all galaxies within a sub-sample. The resulting distribution is then used in place of the original  $n(z)$  during deprojection. We find that the  $r_0$  values increase, as expected from a broader redshift distribution. However, the difference in clustering between the star-forming and passive sub-samples remains, though the difference in implied halo masses is slightly reduced.

This method is very much a simplification and the errors associated with the photometric redshifts are likely to be much more



complex. In particular the errors on the star-forming galaxies' redshifts may deviate significantly from a Gaussian. Photometric redshift codes are known to favour certain redshifts, introducing artificial clumping in redshift space. The spectroscopic redshifts obtained from the UDSz survey will be vital in understanding possible biases arising from using photometric redshifts. We conclude from our current tests, however, that errors in the redshift determination are unlikely to be responsible for the results that we have found.

A further, and potentially important source of error, is that of cosmic sampling variance. In contrast to H08, we have chosen not to take the effects of sampling variance into account. The method employed in H08 consisted of splitting the field into 4 and computing a measurement for each sub-field. This method provides a estimate of the sample variance for a field only one quarter of the size of the original. The ideal method for estimating the sample variance is to repeat these measurements for comparable, independent fields. To facilitate such work in the future we re-define our samples, using simple photometric selection in the Appendix. However, we also note that the clustering of sub-samples at different redshifts are largely uncorrelated, yet we find consistent differences between passive and star-forming galaxies for subsamples with  $z < 1.5$ . We suggest that it is unlikely that we would find such consistent disparity in the clustering results due to cosmic sampling variance alone.

## 5 CONCLUSIONS

We have used the UDS, the deepest contiguous near infrared survey currently available over an area of  $\sim 0.7 \text{ deg}^2$  to investigate the clustering strengths of galaxies over the range  $0 < z < 3$ . Best fitting templates, including a dust contribution, have been measured for each galaxy. From these templates the rest frame U-B colour, absolute K-band magnitude, stellar age and e-folding time of star-formation,  $\tau$ , are derived. These quantities are then used to define 'red' and 'blue' galaxies, a conservative passive sample and active star-forming sample.

Each of these samples are then further sub-divided by redshift and K-band luminosity. Angular correlation function measurements are made for each of these sub-samples and power laws are fit over the scales  $\theta_{lim} < \theta < 0.2$  degrees, where  $\theta_{lim}$  corresponds to  $0.3h^{-1}\text{Mpc}$ . This limited fitting range is used so as to avoid the bias caused by multiple halo occupation (on small scales) and to avoid the scales where the correlation function and integral constraint correction become similar. Using photometric redshift distributions, the angular correlation functions are deprojected to find real space correlation lengths.

We find that the conservatively-defined passive sample is more strongly clustered than the star-forming sample for all luminosities at  $z < 1.5$ . Above this redshift the clustering strengths appear to converge, though we would require greater depth and statistics to make a firm conclusion. Furthermore, by relaxing our strict passive galaxy selection we show that passive galaxies are the most strongly clustered of the 'red' galaxies.

Clustering strength is intimately related to the typical mass of dark matter halo hosting a sample, and K-band luminosity is a reasonable proxy for the stellar mass of a galaxy. We have therefore shown that passive galaxies of a given stellar mass are hosted by more massive halos at  $z < 1.5$ . At higher redshift the convergence of clustering strengths suggests that the red sequence is in the early stages of being populated.

We have also studied how the clustering of passive and star-forming sub-samples compares with those of dark matter halos of

varying mass. The clustering strengths of star-forming galaxies decline towards  $z = 0$  for a given K-band luminosity (stellar mass), and hence are typically found in less massive dark matter halos. This finding is consistent with the wealth of evidence supporting downsizing.

The UDS imaging project is ongoing, and expected to gain at least 1 magnitude in J, H, K depth by 2012, and potentially substantially deeper. This will enable us to extend this work to higher redshift and lower luminosities. In addition, our ongoing spectroscopic programme (UDSz) will provide several thousand spectra over the redshift range probed by this analysis. This will enable a variety of more detailed studies, in addition to substantially improving the reliability of photometric redshifts. The addition of similar deep fields from upcoming surveys (e.g. UltraVISTA) will also allow robust estimates of the sample variance. We therefore anticipate major progress in our understanding of the galaxy populations at the crucial epoch when the red sequence first becomes established.

## ACKNOWLEDGMENTS

WGH would like to extend his thanks to Alfonso Aragón-Salamanca for an extremely useful discussion during the preparation of this work. WGH and SF would also like to acknowledge the support of the STFC during the preparation of this work. IRS acknowledges support from STFC. RJM acknowledges Royal Society funding through the award of a University Research Fellowship. JSD acknowledges the support of the Royal Society through a Wolfson Research Merit award. Finally, we would like to thank the anonymous referee for their very thorough reading of our work and their insightful comments.

## APPENDIX

In this appendix we re-visit the 2-colour selection of Daddi et al. (2004). We aim to derive a series of simple boundaries which can be used to approximate the passive samples used earlier in this work. Our purpose here is to facilitate the reproduction of our results in complementary fields rather than create a robust definition for a passive sample. We choose the  $(B - z')_{AB} - (z' - K)_{AB}$  plane because the pBzK selection of Daddi et al. (2004) is well understood, and also because of the track identified in Lane et al. (2007). This track has colours consistent with the SED of an E/S0 type galaxy, evolved through redshift, and is well separated from the rest of the distribution. It suggests that it may be possible to separate passive and star-forming galaxies over all redshifts with relative ease.

The use of such simple photometric sample definitions may be preferable to full star-formation history fitting when comparing different data sets. In minimising the complexity of selection, the intrinsic differences in the samples should be more apparent and hence a better estimate for cosmic sample variance can be obtained. The colour boundaries outlined below are defined using the Subaru and UKIRT filters. Conversion to other filter sets can be made with reference to Hewett et al. (2006) and Furusawa et al. (2008).

### Samples in the $(B - z') - (z' - K)$ plane

The plane is split into cells,  $0.2 \times 0.2$  in colour, and within each cell the fraction of galaxies that are in the passive sample is computed. Boundaries are chosen to provide a simple selection technique which includes those cells with  $> 50\%$  passive galaxies.

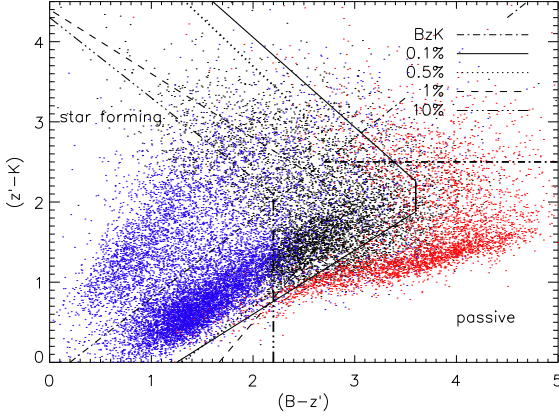


**Figure 7.**  $(B - z')_{AB} - (z' - K)_{AB}$  colour-colour plot for actively star-forming sample (blue points), our ‘conservative’ passive galaxies (red) and those which fall between these criteria (black). Also shown are the commonly used BzK selection criteria of Daddi et al. (2004) and the borders defined in the appendix. Only half of the star-forming points are plotted for clarity.

**Table 1.** Values for the boundary criteria defined in the text.

Co-eff	$0.1\%SFR_i$	$0.5\%SFR_i$	$1\%SFR_i$	$10\%SFR_i$
$\alpha$	0.8	1.0	1.5	...
$\beta$	-1.0	-1.3	-2.5	...
$\gamma$	3.6	...	...	2.2
$\delta$	-1.4	-1.2	-0.8	-1.0
$\epsilon$	7.3	6.1	4.4	4.3

These borders are shown in Figure 7 together with the conservative passive sample and star-forming samples used in the main body of this paper. The boundaries for each sample are:

$$\begin{aligned}
 & (z' - K)_{AB} < \alpha(B - z')_{AB} + \beta \\
 \text{or } & (B - z')_{AB} > \gamma \\
 \text{or } & (z' - K)_{AB} > \delta(B - z')_{AB} + \epsilon;
 \end{aligned} \tag{6}$$

where the values for  $\alpha, \beta, \gamma, \delta$  and  $\epsilon$  are given in table 1.

These 2-colour-defined passive samples include all galaxies in the relevant region regardless of their best-fit age, U-B colour or SFR. The number of objects in each sample are 5438, 7287, 8986 and 12242 respectively, and the number of objects in the star-forming sample is 20645.

The clustering properties of these galaxy samples were treated in the same way as those in the main body of this paper. In each case the properties of galaxies selected by the photometrically-defined borders, shown in Figure 7, reflect those of the intended population: the majority of sub-samples having very similar clustering strengths. Each of the conclusions drawn previously are equally applicable to these photometrically-selected samples.

The border-defined passive samples include slightly larger numbers of galaxies than the more physically motivated selections presented earlier in this paper. The additional galaxy numbers enable measurements beyond  $z = 2$  for some of these samples. Though highly uncertain, these measurements indicate equivalence of clustering strength at  $z > 2$ , as was suggested in section 4.

## REFERENCES

- Adelberger K. L., Steidel C. C., Shapley A. E., Hunt M. P., Erb D. K., Reddy N. A., Pettini M., 2004, *ApJ*, 607, 226
- Blain A. W., Chapman S. C., Smail I., Ivison R., 2004, *ApJ*, 611, 725
- Bond J. R., Cole S., Efstathiou G., Kaiser N., 1991, *ApJ*, 379, 440
- Brammer G. B., et al., 2009, *ApJ*, 706, L173
- Bruzual G., Charlot S., 2003, *MNRAS*, 344, 1000
- Bundy K., et al., 2006, *ApJ*, 651, 120
- Calzetti D., Armus L., Bohlin R. C., Kinney A. L., Koornneef J., Storchi-Bergmann T., 2000, *ApJ*, 533, 682
- Carlberg R. G., Cowie L. L., Songaila A., Hu E. M., 1997, *ApJ*, 484, 538
- Casali M., et al., 2007, *A&A*, 467, 777
- Cimatti A., Daddi E., Renzini A., 2006, *A&A*, 453, L29
- Cimatti A., et al., 2008, *A&A*, 482, 21
- Cirasuolo M., et al., 2007, *MNRAS*, 380, 585
- Cirasuolo M., McLure R. J., Dunlop J. S., Almaini O., Foucaud S., Simpson C., 2010, *MNRAS*, 401, 1166
- Coil A. L., Newman J. A., Cooper M. C., Davis M., Faber S. M., Koo D. C., Willmer C. N. A., 2006, *ApJ*, 644, 671
- Coil A. L., et al., 2008, *ApJ*, 672, 153
- Conselice C. J., O’Neil K., Gallagher J. S., Wyse R. F. G., 2003, *ApJ*, 591, 167
- Conselice C. J., et al., 2007, *ApJ*, 660, L55
- Conselice C. J., et al., 2007, *MNRAS*, 381, 962
- Cowie L. L., Songaila A., Hu E. M., Cohen J. G., 1996, *AJ*, 112, 839
- Daddi E., et al., 2004, *ApJ*, 617, 746
- Dressler A., 1980, *ApJ*, 236, 351
- Dye S., et al., 2006, *MNRAS*, 372, 1227
- Einasto M., 1991, *MNRAS*, 252, 261
- Farrah D., et al., 2006, *ApJ*, 641, L17
- Foucaud S., et al., 2007, *MNRAS*, 376, L20
- Foucaud S., et al., 2010, *MNRAS*, in press - astro-ph/1003.2755
- Franx M., et al., 2003, *ApJ*, 587, L79
- Fujita Y., Nagashima M., 1999, *ApJ*, 516, 619
- Furusawa H., et al., 2008, *ApJS*, 176, 1
- Gunn J. E., Gott J. R. I., 1972, *ApJ*, 176, 1
- Hartley W. G., et al., 2008, *MNRAS*, 391, 1301
- Heinis S., et al., 2007, *ApJS*, 173, 503
- Hewett P. C., Warren S. J., Leggett S. K., Hodgkin S. T., 2006, *MNRAS*, 367, 454
- Hughes D. H., et al., 1998, *Natur*, 394, 241
- Ilbert O., et al., 2006, *A&A*, 457, 841
- Jing Y. P., 1998, *ApJ*, 503, L9
- Kong X., et al., 2006, *ApJ*, 638, 72
- Landy S. D., Szalay A. S., 1993, *ApJ*, 412, 64
- Lane K. P., et al., 2007, *MNRAS*, 379, L25
- Lawrence A., et al., 2007, *MNRAS*, 379, 1599
- Le Fèvre O., et al., 2005, *A&A*, 439, 845
- Lilly S. J., Longair M. S., 1984, *MNRAS*, 211, 833
- Lilly S. J., Eales S. A., Gear W. K. P., Hammer F., Le Fèvre O., Crampton D., Bond J. R., Dunne L., 1999, *ApJ*, 518, 641
- Lilly S. J., et al., 2007, *ApJS*, 172, 70
- Limber D. N., 1954, *ApJ*, 119, 655
- Lonsdale C. J., et al., 2003, *PASP*, 115, 897
- Madau P., 1995, *ApJ*, 441, 18
- Madgwick D. S., et al., 2003, *MNRAS*, 344, 847
- Magliocchetti M., Maddox S. J., 1999, *MNRAS*, 306, 988
- Magliocchetti M., et al., 2008, *MNRAS*, 383, 1131

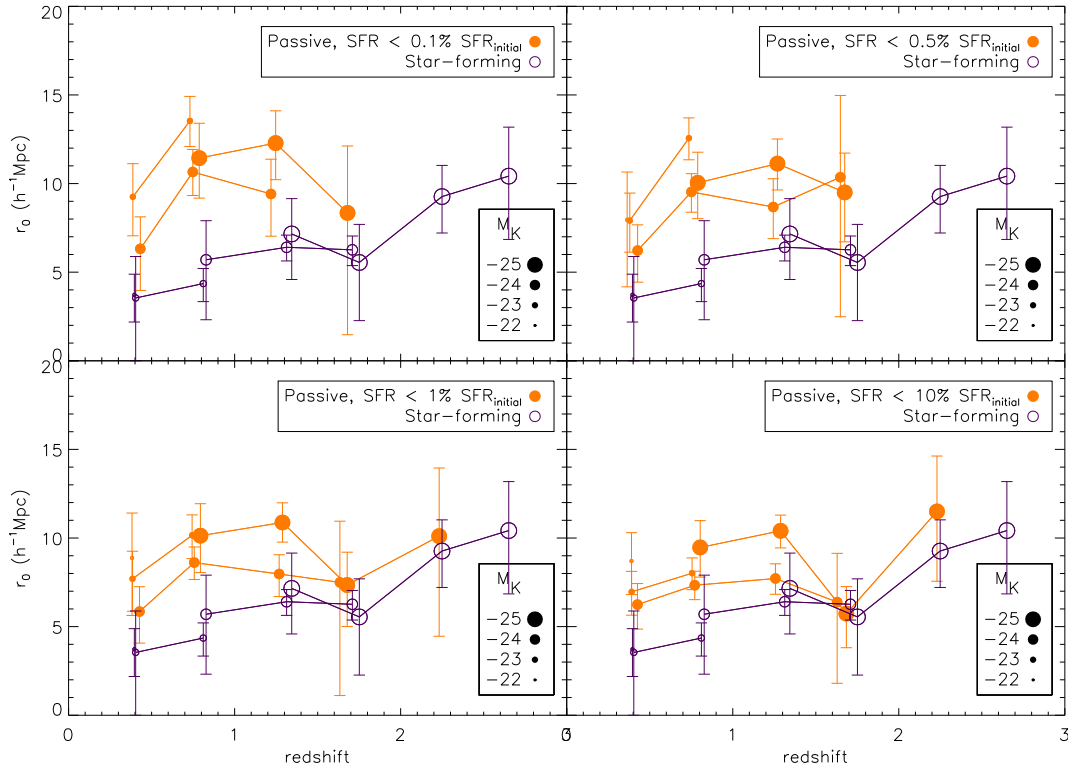


**Figure 8.** Clustering strengths of the 2-colour-defined galaxies. The symbols have the same meanings as in Figure 4. The values for  $r_0$  are largely consistent with those in Figure 4. Use of the boundaries defined for these samples should therefore yield measurements suitable for comparison with our main results.

McCarthy P. J., et al., 2004, *ApJ*, 614, L9  
 McCracken H. J., Ilbert O., Mellier Y., Bertin E., Guzzo L., Arnouts S., Le Fèvre O., Zamorani G., 2008, *A&A*, 479, 321  
 Meneux B., et al., 2006, *A&A*, 452, 387  
 Meneux B., et al., 2009, *A&A*, 505, 463  
 Meneux B., et al., 2009, arXiv:0906.1807  
 Mo H. J., White S. D. M., 1996, *MNRAS*, 282, 347  
 Mo H. J., White S. D. M., 2002, *MNRAS*, 336, 112  
 Norberg P., et al., 2002, *MNRAS*, 332, 827  
 Peebles P. J. E., 1980, *The Large-Scale Structure of the Universe*. Princeton University Press, Princeton, NJ  
 Pozzetti L., Mannucci F., 2000, *MNRAS*, 317, L17  
 Press W. H., Schechter P., 1974, *ApJ*, 187, 425  
 Roche N., Eales S. A., 1999, *MNRAS*, 307, 703  
 Roche N. D., et al., 2002, *MNRAS*, 337, 1282  
 Roche N. D., Dunlop J., Almaini O., 2003, *MNRAS*, 346, 803  
 Sekiguchi K., et al., 2005, in Renzini A., Bender R., eds, *Multi-wavelength Mapping of Galaxy Formation and Evolution Multi-wavelength Observations of the Subaru/XMM-Newton Deep Field*.  
 Sheth R. K., Mo H. J., Tormen G., 2001, *MNRAS*, 323, 1  
 Swinbank A. M., Chapman S. C., Smail I., Lindner C., Borys C., Blain A. W., Ivison R. J., Lewis G. F., 2006, *MNRAS*, 371, 465  
 Toft S., et al., 2007, *ApJ*, 671, 285  
 Visvanathan N., Sandage A., 1977, *ApJ*, 216, 214  
 Warren S. J., et al., 2007, *MNRAS*, 375, 213  
 Weiß A., et al., 2009, *ApJ*, 707, 1201  
 Williams R. J., Quadri R. F., Franx M., van Dokkum P., Labbé I., 2009, *ApJ*, 691, 1879

Wolf C., Gray M. E., Meisenheimer K., 2005, *A&A*, 443, 435  
 Yamada T., et al., 2005, *ApJ*, 634, 861  
 York D. G., et al., 2000, *AJ*, 120, 1579  
 Zehavi I., et al., 2005, *ApJ*, 630, 1  
 Zirm A. W., et al., 2007, *ApJ*, 656, 66  
 Zucca E., et al., 2006, *A&A*, 455, 879